



# Use of Selective Laser Melting (SLM) as a Replacement for Pressure Die Casting Technology for the Production of Automotive Casting

J. Piekło, A. Garbacz-Klempka\*

AGH University of Science and Technology, Faculty of Foundry Engineering,  
Reymonta 23 Str., 30-059 Kraków, Poland

\* Corresponding author. E-mail address: [agarbacz@agh.edu.pl](mailto:agarbacz@agh.edu.pl)

Received 22.12.2020; accepted in revised form 02.04.2021

## Abstract

Selective laser melting is one of the additive manufacturing technologies that is used to produce complex-shaped components for applications in the automotive industry. The purpose of the changes in the design, technology, and material tests was to make a steering gear housing using the SLM method. The steering gear housing was produced by the pressure casting method using an AlSi9Cu3(Fe) alloy. The construction of this housing is adapted to the specifics of left-hand traffic. The change in technology was related to the change of the position of the steering system from right-hand to left-hand and the demand for a limited number of gear housings. It was necessary to make a virtual model of the housing on the basis of the part that was removed from the vehicle. In SLM technology, the AlSi10Mg aluminum alloy was used as a raw material in the form of CL 32Al gas-atomized powder. After the SLM process was completed, the housings were subjected to heat treatment. The AlSi10Mg alloy fabricated by the SLM method after heat treatment is characterized by good plasticity and an average value of tensile strength. The last stage was to check the geometry of the SLM housing with a 3D scanner. As a result, a map of the dimensional deviations from the nominal values was obtained. This data was used to modify the CAD model before the next fabrication process.

The use of 3D printing technology allowed for the quick production of elements. The time to develop the technology and the production of the first two gear housings based on a 3D model was seven days.

**Keywords:** Additive manufacturing (AM), Selective laser melting (SLM), Automotive casting, AlSi10Mg, Mechanical properties, Microstructure

## 1. Introduction

Selective laser melting (SLM) is one of the additive manufacturing (AM) technologies that is used to produce complex-shaped components in several structural alloys for

applications in the automotive, aerospace, and biomedical sectors. The SLM process is one of the powder bed fusion AM technologies according to ISO/ASTM 52900 [1]. The SLM process directly produces metal parts layer by layer from 3D CAD data by the laser melting of thin layers of metal powder with a laser beam [2]. With regard to the SLM state-of-the-art

process and the cost efficiency of cast aluminum alloys, SLM technology is not suited for series production. However, this method is cost-effective for short series of parts. The final properties of the parts (such as the densification microstructure and mechanical properties) depend on SLM process factors and variables – the process parameters and powder properties [3]. Gas-atomized powders are generally preferred for the SLM process because of their spherical shapes, which causes good powder flowability. Good flowability is required to achieve powder layers with a constant thickness, which favors a uniform laser beam absorption and eliminates any melt track instability effects [4-5]. Producing parts from powders of aluminum alloys by the SLM method face some difficulties as compared to other alloys due to their high reflectivity, high thermal conductivity, and stability of the oxide layer. The correct determination of the SLM process parameters increases the density of the material and increases its strength properties. Optimal laser energy in the SLM process is defined by many authors using the equation (1) [6]:

$$E = \frac{P}{V \cdot h \cdot t} \quad (1)$$

where:

E – energy density (J/mm<sup>3</sup>);

P – laser power (J);

V – scanning speed (mm/s);

h – scan line spacing or hatching distance (mm);

t – layer thickness (mm).

By selecting the appropriate laser power and scanning speed, a process window is determined [7]. Using the correct strategy (which is the geometrical pattern that the laser beam follows during the hatching to melt and consolidate a section onto a layer) allows the part to be made without defects and free from distortion warping, porosities, and anisotropy [8]. The correctly selected process parameters and scan strategies can produce parts with a density of 99.8% [9]. The building orientation of the part affects the microstructural evolution and may result in its consequent anisotropy [9]. The microstructure of the AlSi alloy obtained by the SLM method consists of a cellular-dendritic structure of an  $\alpha$ -Al phase and a network of eutectic Si phases along the boundary that surrounds the  $\alpha$ -Al phase. The dimensions of the Al cellular dendrites corresponded to 500-1000 nm; that is, much lower values than those of the cast [10]. As in the case of the castings, the SLM material is heat-treated. The applied heat (heat up to 300°C, maintain a temperature of 300°C for 2 hours [11], decrease heat to 240°C over 1 hour, and maintain temperature for 6 hours) allow the components to cool down to 100°C in the oven [12]. According to [13], the tensile strength of the AlSi10Mg alloy that is fabricated by selective laser melting is 434 ± 11 MPa, while the elongation is 5.3 ± 0.2%. The applied stress relief annealing reduces the strength to 168 ± 2 MPa and even increases the elongation value to 23.7 ± 8.7% when an as-built sample is solution-treated at 550°C for 2 h. An AlSi10Mg alloy fabricated by SLM also has a high hardness (127 ± 3 HV [14]), high fatigue resistance [15], and better strength and elongation properties

than a die-cast alloy of a similar composition; also, the creep results show a better rupture life than the cast alloy [9,16-17].

## 2. Materials and methods

Aluminum alloy AlSi10Mg in the form of CL 32Al gas-atomized powder produced by AP&C-a GE Additive Company was used as the raw material. The chemical composition of the powder (determined on the basis of spectroscopic tests) is listed in Table 1.

Table 1.

Chemical composition (%wt.) of studied powder.

Chemical composition (%wt.)							
Si	Fe	Mn	Mg	Zn	Cu	Ti	Al
10.20	0.21	0.11	0.35	0.05	0.02	0.09	balance

Figures 1 and 2 shows the SEM morphology of the powder, and Figure 3 shows its size distribution as measured by a Fritsch Analysette 22 NanoTech laser-scattering particle size analyzer. The powder that was previously used to print the SLM parts was used in the research.

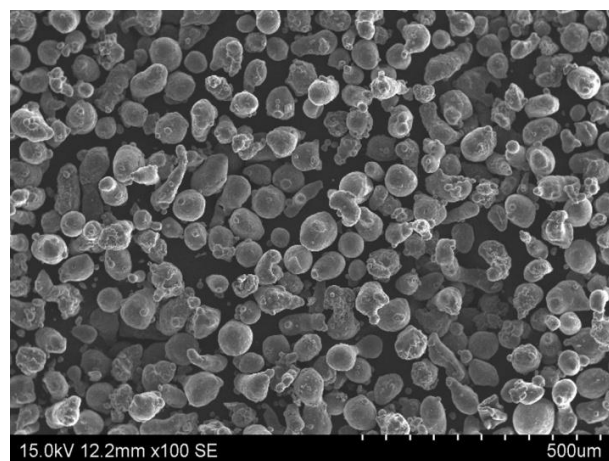


Fig. 1. SEM morphology of AlSi10Mg powder

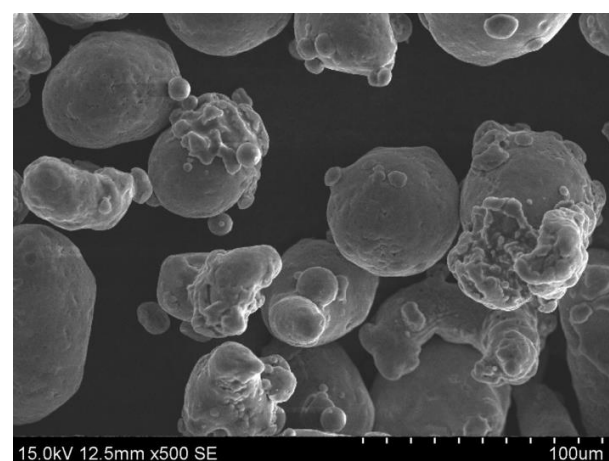


Fig. 2. SEM morphology of AlSi10Mg powder

The powder particles had a median particle size of cumulative volume distribution  $x_{50,3} = 63.14 \mu\text{m}$ . The minimum and maximum particle sizes were  $x_{\min} = 20 \mu\text{m}$  and  $x_{\max} = 110 \mu\text{m}$  and are spherical or quasi-spherical in shape (Figures 1-2). This shape allows the particles to flow without hindrance during deposition. The samples for testing and automotive steering gear housing were made using a Concept Laser X Line 2000R device having a working chamber with dimensions of 800 x 400 x 500 mm.

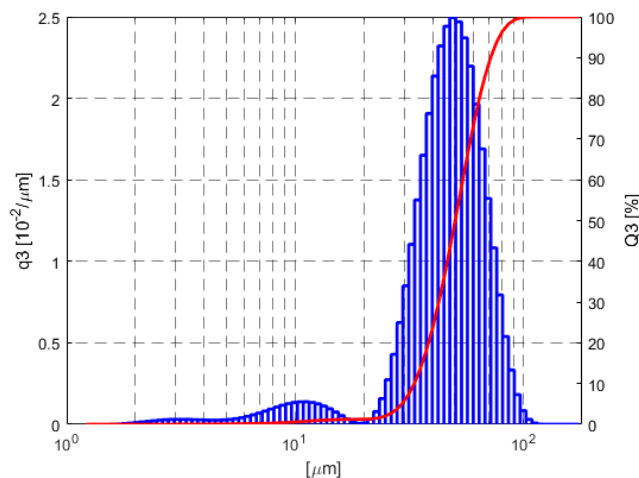


Fig. 3. Size distribution of studied AlSi10Mg powder

The material was printed in a nitrogen atmosphere using the two fiber-lasers-following parameters collected in Table 2. A meander scanning strategy was used, which assumes that the direction of the laser beam is changed by an angle of  $67^\circ$  for each layer.

Table 2.

SLM proces parameters

SLM parameter	Solid section	Surface	Support
Laser power (W)	950	420	400
Laser speed (mm/s)	2400	700	2250
Laser beam diameter ( $\mu\text{m}$ )	200	100	100
Layer thickness ( $\mu\text{m}$ )	50	50	50
Hatch space (mm)	0.17	-	-
Laser Energy density ( $\text{J}/\text{mm}^3$ )	65.9	120.0	35.6

The relative density  $\rho_r$  of the fabricated specimens was measured by formula  $\rho_r = (m_0\rho_1)/(m_0\rho_0 - m_1\rho_0)$  according to Archimedes' principle, in which  $m_0$ ,  $\rho_0$ ,  $m_1$ , and  $\rho_1$  are the AlSi10Mg alloy specimen's weight in air, its theoretical full-density ( $2.67 \text{ g}/\text{cm}^3$ ), its weight when submerged in water, and the density of the applied water under normal atmospheric pressure, respectively. The relative density of the fabricated specimens reached 99.2%. Strength tests were carried out on samples with a measured length of 28 mm and diameter of 5 mm. The axis of each sample was perpendicular to the plane of the base plate of the SLM device. Such a position of the printed part in relation to the base plate is usually least-favorable in terms of the strength properties of the obtained material. To measure the elongation, an MTS extensometer with a 25-mm base was used. A static tensile test was carried out according to ISO 6892-1 at an ambient temperature on

an MTS 810 testing system. Metallographic tests of the microsections and fractures were performed using a NIKON ECLIPSE metallographic microscope with a DsFi1 camera that allowed for digital image analysis as well as a HITACHI S-3400N scanning electron microscope. The heat treatment of the samples and automotive steering gear housing consisted of heating up to  $240^\circ\text{C}$  within 1 hour, heating in an oven at  $240^\circ\text{C}$  for 6 hours, and cooling down to  $100^\circ\text{C}$  over 1 hour. The automotive steering gear housing was scanned using a Hexagon 3D Stereo Scan Neo R8 scanner. The maximum working area of the scanner was 500 x 500 mm. The scanner enabled the mapping of the object with an accuracy of  $12 \mu\text{m}$ . Using the Solid Works Premium software, fully parametric and editable 3D models were made from the scan files.

### 3. Description of the research results

The purpose of the changes in the design, technology, and material tests was to make the steering gear housing by using the SLM method. The steering gear housing was produced by the pressure casting method from the AlSi9Cu3(Fe) alloy. The construction of this housing was adapted to the specificity of left-hand traffic. The change in technology was related to the change of the position of the steering system from right-hand to left-hand as well as the demand for a limited number of gear housings. There was no drawing documentation of the product; therefore, it was necessary to make a virtual model of the housing on the basis of the part that was removed from the vehicle. Due to the small number of details (20 pieces), making them by casting was not profitable. The use of 3D printing technology allowed for the quick production of the parts. The time to develop the technology and the production of the first two gear housings based on the 3D model was seven days.

#### 3.1. Model of the housing - preparation and manufacturing

The first step was to make a CAD model of the steering gear housing (Figure 4a) with machining allowances for finishing. The housing model was made on the basis of a cast that was removed from a vehicle and delivered by the customer. The housing model to be fabricated using the SLM method was prepared using the Materialize Magics software. This software allows us to set the detail in the working area of the machine, generate support structures (Figure 4b), and prepare a control program for the machine. The gear housing that was fabricated using the SLM method (Figure 4c) was made on an X-Line 2000 machine manufactured by Concept Laser. After the SLM process was completed, the housings were subjected to stress relief annealing consisted of heat up to  $240^\circ\text{C}$  and maintained for 6 hours. Then, the covers were cut from the base plate on which the fabrication was made. The support structures were removed (Figure 4d), and the finished detail was cleaned. The last stage was to check the geometry of the SLM housing with a 3D scanner. As a result, a map of the dimensional deviations from the nominal values was obtained.

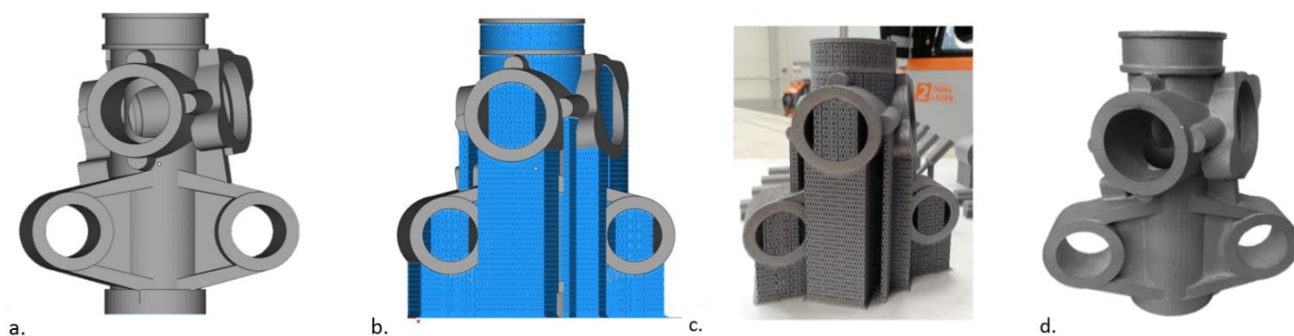


Fig. 4. CAD model and SLM part of the automotive steering gear housing: a - CAD model of the gear housing, b - CAD model of the gear housing with added support structures, c- the gear housing with support structures fabricated using the SLM method, d - cleaned gear housing fabricated using the SLM method

This data was used to modify the CAD model before the next fabrication process in order to obtain dimensions of the steering gear housing that were as close as possible to the assumed nominal dimensions of this model.

### 3.2. Accuracy analysis

The housing parts that were fabricated using the SLM method were heat-treated and cut from the base plate. Accuracy

tests performed with the use of a 3D scanner revealed any differences between the dimensions of the CAD model and the finished part. Deviations from the assumed values of the dimensions for the first printed part ranged from -0.6 to 0.4 mm. Based on the results of the deviations from the nominal dimensions presented in Figure 5, the dimensions of the CAD model were corrected. X-rays of the gearbox casing that was fabricated using the SLM method showed no porosity nor other internal defects of the material (Figure 6).

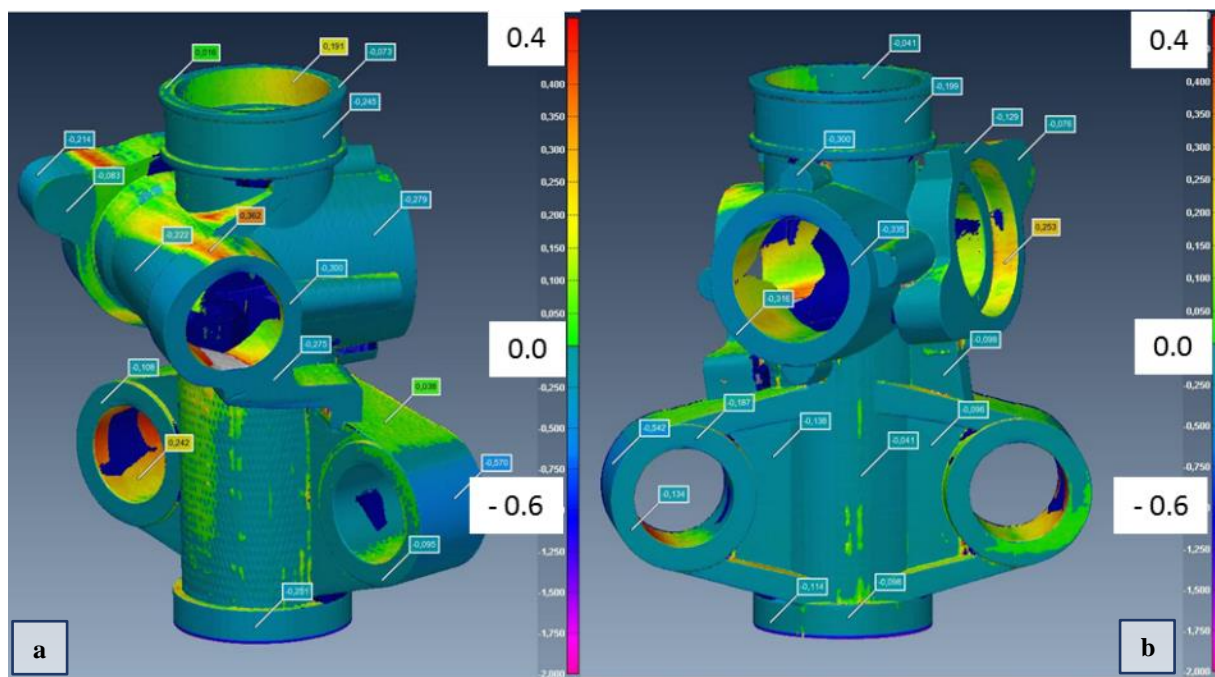


Fig. 5. Deviations from the nominal dimensions of the first steering gear housing fabricated using the SLM method; a, b - two different viewing directions



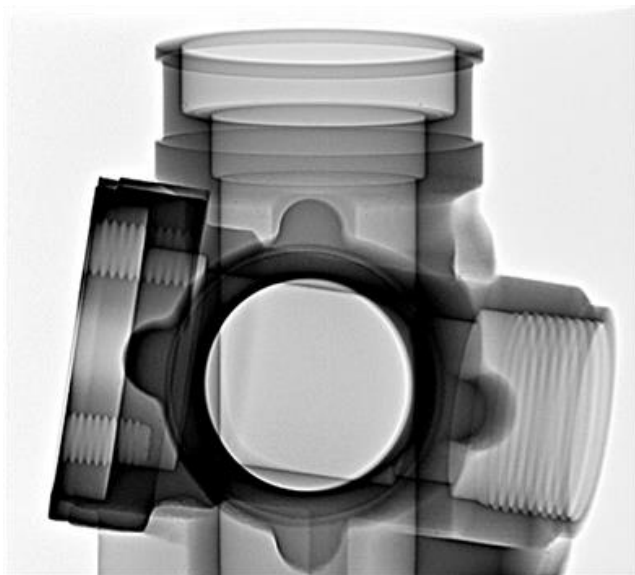


Fig. 6. X-ray image of steering gear housing fabricated by SLM method

### 3.3. Microstructure analysis

Along with the gear housing that was fabricated using the SLM method, samples for static tensile strength tests were also created. The main axes of the samples were directed perpendicular to the plane of the base plate. In this position in relation to the base plate, the printed samples have the lowest strength and elongation. This phenomenon can be explained by the perpendicular direction of the tensile force during the static tensile test in relation to the fusion surface of the powder layers. The image of the microstructure of the AlSi10Mg alloy is shown in Figure 7. The parallel view of the direction of the laser scanning path shown in Figures 7a and 7c revealed the presence of scanning paths in the form of parallel lines. The perpendicular view to the direction of the laser scanning path shown in Figures 7b and 7d revealed semi-circular cross-sections of the scanning paths that overlap, forming the characteristic pattern. This semi-circular form resulted from the formation of a “melting pool” in the area where the part of the underlying substrate and new layer of applied powder were melted with the laser beam. The overlapping scanning paths that are visible in Figures 7b and 7d prevented the formation of any possible alloy discontinuity. The changes in the scanning direction in the adjacent layers were meant to prevent excessive stress increase.

The directional cooling and very rapid solidification caused three different sizes of the cellular – dendritic structures. In the middle of the melt pool, a fine grain structure can be observed. Adjacent to the melting pool boundary and in the region between the two overlapping melt pools, the grains are coarser (Figure 8).

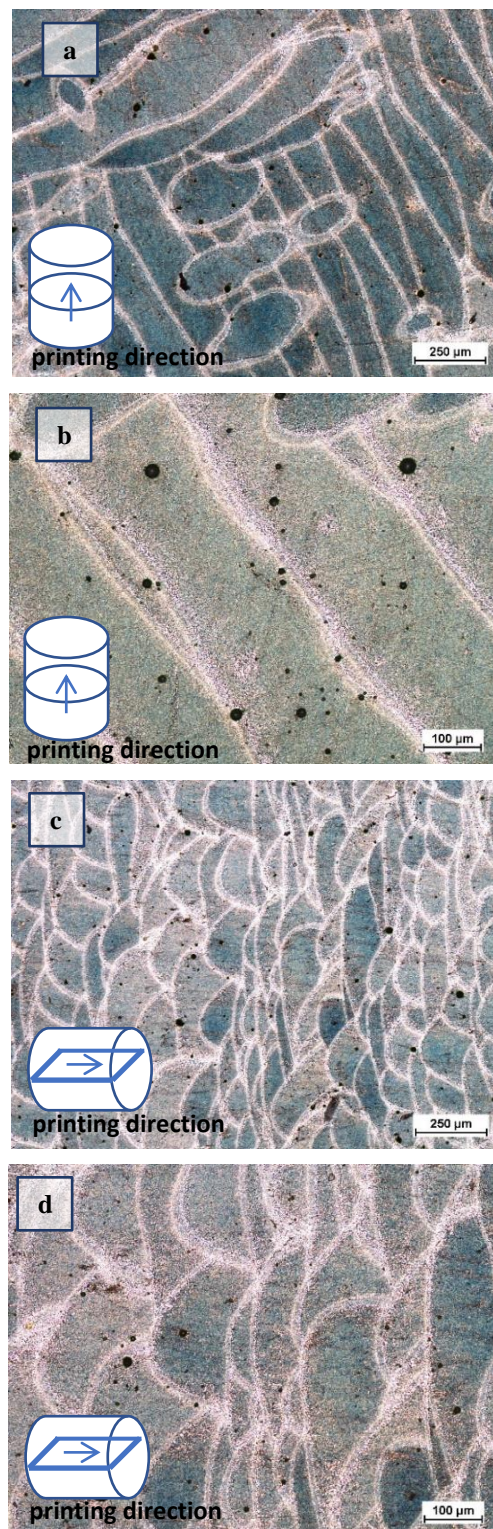


Fig. 7. Images of fabricated using the SLM method AlSi10Mg alloy microstructure in as-built condition after etching with nital reagent: a,c – view direction perpendicular to direction of laser scanning path; b, d – view direction parallel to direction of laser scanning path

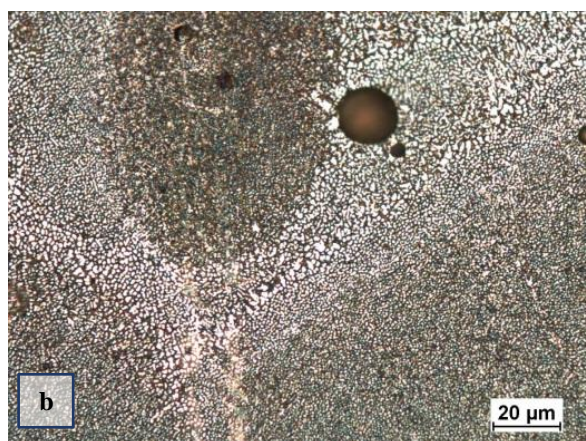


Fig. 8. Images of AlSi10Mg alloy microstructure fabricated using SLM method in as-built condition after etching with nital reagent (optical microscope); it is possible to observe different sizes of cellular-dendritic structures

### 3.4. Tensile test and fracture surface analysis

Figure 9 shows typical graphs of the elongation function  $A$  – the stress obtained during the tensile tests of the material after stress relief annealing consisting of heating up to 240°C and maintained for 6 hours. The AlSi10Mg alloy fabricated by the SLM method is characterized by good plasticity and an average value of tensile strength after stress relief annealing. The average values of the tensile strength UTS, yield strength  $R_{p0.2}$ , Young's modulus  $E$ , and elongation  $A$  determined on the basis of the static tensile test carried out on five samples are presented in Table 3.

Table 3.

Strength properties of the fabricated SLM method AlSi10Mg alloy after stress relief annealing determined in the static tensile test

UTS (MPa)	$R_{p0.2}$ (MPa)	$E$ (GPa)	$A$ (%)
271 ( $\pm 15$ )	160 ( $\pm 20$ )	74 ( $\pm 3$ )	7.15 ( $\pm 2.10$ )

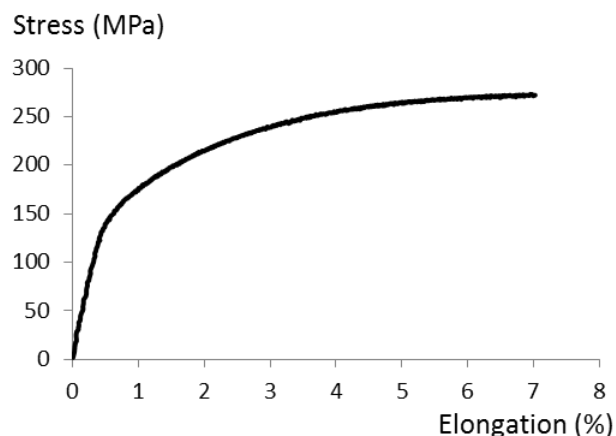


Fig. 9. Typical tensile curve of fabricated AlSi10Mg alloy using SLM method after performed stress relief heat treatment

## 4. Discussion of the results

Due to the replacement of the pressure casting technology of the steering gear housing with the SLM method (Figure 10), another grade of alloy was used for its production. The AlSi9Cu3(Fe) alloy is a typical alloy that is used in pressure die casting. On the other hand, the AlSi10Mg alloy is very often used for the production of parts by the SLM method due to its good weldability, high strength properties, and corrosion resistance. AlSi10Mg is a eutectic composition of the Al-Si system. Due to the non-equilibrium solidification conditions caused by the increased undercooling in front of the solid-liquid interface, the eutectic is considered to be a fine pseudo-eutectic microstructure. The eutectic of the alloy fabricated by the SLM method contains more Si and Al than a cast alloy of the same composition. Tests of the microstructure of the alloy produced by the SLM method confirmed the large fragmentation of the microstructure that was caused by very fast cooling and the directionality of the structure of the raw alloy, which is removed only after the thermal treatment. The strength of the alloy depends to a large extent on the parameters of the performed heat treatment. The conventional method of the heat treatment of cast Al-Si-Mg alloys consists of supersaturation within a temperature range of 450°C to 575°C, followed by rapid cooling and aging within a temperature range of 93°C to 245°C. Al-Si-Mg alloys obtained by the SLM method are not supersaturated but only aged. After the stress relief heat treatment process (consisting of heating up to 240°C and maintained for 6 hours), the SLM alloy obtained a strength of 271 MPa and an elongation of 7.15%.





Left-hand drive-SLM Part      Right-hand steering system (die-cast)  
 Fig. 10. Off-road vehicle steering gear housings: a – SLM technology; b - die-cast.

The support structure increases the range of the SLM manufacturable geometries and has several technical functions, such as physical support to slender and overhanging geometries, increased heat transfer, and physical resistance to bulk structural deformation and thermal distortion. The support structure should be frangible to allow for easy removal and minimize post processing [18]. To support the steering gear housing model, a commercial method for generating a support structure was used (Figure 4c). The shape deviations for the trial print of the housing are shown in Figure 5. After the shape correction in the CAD model, these were reduced to  $\pm 95 \mu\text{m}$ . According to Technical Data by EOS typical achievable part accuracy, these should not exceed  $\pm 20 \mu\text{m}$  on average for parts made with the SLM method from maraging steel powder with dimensions that are smaller than  $80 \times 80 \text{ mm}$ ; for parts with dimensions that are greater than  $80 \times 80 \text{ mm}$ , this should not exceed about  $\pm 50 \mu\text{m}$  [19]. On the other hand, the optimal dimensional tolerances of the castings quoted in article for pressure casting technology are from  $50$  to  $200 \mu\text{m}$  for dimensions that are within a range of  $30$  to  $50 \text{ mm}$  [20].

## 5. Conclusions

Additive AM technologies can be used as a tool for making tooling for permanent, metal [21], and disposable ceramic casting molds [22]. In the case of a short series of manufactured parts, the SLM method can be competitive with foundry technologies, especially when the detail is to be made in a metal mold or pressure mold. Due to their very fine microstructures, AlSi10Mg materials that are produced by SLM technologies possess UTS, Young's modulus, and elongation values that are comparable to a casted AlSi10Mg alloy. The dimensional accuracy of SLM parts is comparable

to the tolerances of pressure die castings, while the surface structure depends strongly on the position of the SLM part on the build plate due to its layer-wise building. Hence, the roughness of the SLM part varies (with  $R_a = 9\text{-}20 \mu\text{m}$ ). The surface roughness of SLM parts is greater than that of pressure castings, for which  $R_a = 0.6$  to  $2.5 \mu\text{m}$  (or  $2.5$  to  $5 \mu\text{m}$  in the case of long mold operation) [23].

The use of 3D printing technology allowed for quick production of parts. The time to develop the technology and the production of the first two gear housings based on a 3D model was 7 days.

At the time of submitting the article for printing, the trial phase of the housing was started.

## Acknowledgements

The research was supported by National Center for Research and Development in the framework of "Ścieżka dla Mazowsza". Program under the project: "Development and commissioning of an innovative die-casting technology with the use of targeted crystallization used to improve the quality of the structure and surface of small-sized details" no MAZOWSZE / 0011/19.

Thanks to the RCiT company from Radom, Poland for their cooperation and the possibility of making the printed parts of the casting moulds and the samples necessary for the implementation of our research.

## References

- [1] *Additive Manufacturing – General Principles – Terminology* (2015). ISO/ASTM 2900:2015. BSI: London, UK.
- [2] Frazier, W.E. (2014). Metal additive manufacturing: A review. *Journal of Materials Engineering and Performance*. 23, 1917-1928. DOI: 10.1007/s11665-014-0958-z.
- [3] Sercombe, T.B. & Li, X. (2016). Selective laser melting of aluminum and aluminum metal matrix composites. *Review. Materials Technology*. 31(2), 77-85. DOI: 10.1179/1753555715Y.0000000078.
- [4] Yadroitsev, I., Yadroitsava, I., Bertrand, P. & Smurov, I. (2012). Factor analysis of selective laser melting process parameters and geometrical characteristics of synthesized single tracks. *Rapid Prototyping Journal*. 18(3), 201-208. DOI: 10.1108/13552541211218117.
- [5] Olakanmi, E.O. (2013). Selective laser sintering/melting (SLS/SLM) of pure Al, Al-Mg, and Al-Si powders: Effect of processing conditions and powder properties. *Journal of Materials Processing Technology*. 213(8), 1387-1405. DOI: 10.1016/j.jmatprotec.2013.03.009.
- [6] Gibson, I., Rosen, D.W. & Stucker, B. (2010). *Additive Manufacturing Technologies, Rapid Prototyping to Direct Digital Manufacturing*. Springer New York Heidelberg Dordrecht London. DOI: 10.1007/978-1-4419-1120-9.

- [7] Kempen, K., Thijs, L., Van Humbeeck, J. & Kruth, J.P. (2015). Processing AlSi10Mg by selective laser melting: parameter optimisation and material characterization. *Materials Science and Technology*. 31(8), 917-923, DOI: 10.1179/1743284714Y.0000000702.
- [8] Aboulkhair, N.T., Everitt, N.M., Ashcroft, I. & Tuck, C.N. (2014). Reducing porosity in AlSi10Mg parts processed by selective laser melting. *Additive Manufacturing*. 1-4, 77-86. DOI: 10.1016/j.addma.2014.08.001.9.
- [9] Read, N., Wang, W. & Essa, K. & Attallah, M. (2015). Selective laser melting of AlSi10Mg alloy: Process optimisation and mechanical properties development. *Materials & Design*. 65, 417-424. DOI: 10.1016/J.MATDES.2014.09.044.
- [10] Lam, L.P., Zhang, D.Q., Liu, Z.H. & Chua, C.K. (2015). Phase analysis and microstructure characterisation of AlSi10Mg parts produced by Selective Laser Melting. *Virtual and Physical Prototyping*. 10 (4), 207-215. DOI: 10.1080/17452759.2015.1110868.
- [11] EOS Material data sheet, EOS Aluminium AlSi10Mg. [www.eos.info/03\\_system-related-assets/material-related-contents/metal-materials-and-examples/metal-material-datasheet/aluminium/alsi10mg-9011-0024-m400\\_flexline\\_material\\_data\\_sheet\\_03-18\\_en.pdf](http://www.eos.info/03_system-related-assets/material-related-contents/metal-materials-and-examples/metal-material-datasheet/aluminium/alsi10mg-9011-0024-m400_flexline_material_data_sheet_03-18_en.pdf).
- [12] Concept Laser a GE Additive Company, CL 32 Al Aluminium alloy. [www.ge.com/additive/sites/default/files/2018-12/CL\\_32AL\\_DS\\_DE\\_US\\_v1.pdf](http://www.ge.com/additive/sites/default/files/2018-12/CL_32AL_DS_DE_US_v1.pdf).
- [13] Li, W., Li, S., Liu, J., Zhang, Y., Wei, Q., Yan, C. & Shi, Y. (2016). Effect of heat treatment on AlSi10Mg alloy fabricated by selective laser melting: Microstructure evolution, mechanical properties and fracture mechanism. *Materials Science and Engineering A*. 663, 116-125. DOI: 10.1016/j.msea.2016.03.088.
- [14] Thijs, L., Kempen, K., Kurth, J.P. & Van Humbeeck, J. (2013). Fine-structured aluminium products with controllable texture by selective laser melting of pre-alloyed AlSi10Mg powder. *Acta Materialia*. 61(5), 1809-1819. DOI: 10.1016/j.actamat.2012.11.052.
- [15] Brandl, E., Heckenberger, U., Holzinger, V. & Buchbinder, D. (2012). Additive manufactured AlSi10Mg samples using Selective Laser Melting (SLM): Microstructure, high cycle fatigue, and fracture behavior. *Materials & Design*. 34, 159-169. DOI: 10.1016/j.matdes.2011.07.067.
- [16] Piekło, J., Garbacz-Klempka, A., Żuczek, R. & Małysza, M. (2019). Computational modeling of fracture toughness of Al-Si, and Al-Zn-Mg-Cu alloys with detected porosity. *Journal of Materials Engineering and Performance*. 28, 1373-1381. DOI: 10.1007/s11665-019-03899-2.
- [17] Zych, J., Piekło, J., Maj, M., Garbacz-Klempka, A. & Piękoś, M. (2019). Influence of structural discontinuities on fatigue life of 4XXX0-series aluminum alloys. *Archives of Metallurgy and Materials*. 64(2), 765-771. DOI: 10.24425/amm.2019.127611.
- [18] Leary, M., Maconachie, T., Sarker, A. & Faruque, O. (2019). Mechanical and thermal characterisation of AlSi10Mg SLM block support structures. *Materials and Design*. 183(5), 108-138. DOI: 10.1016/j.matdes.2019.108138.
- [19] EOS Material data sheet, EOS MaragingSteel MS1. [www.eos.info/03\\_system-related-assets/material-related-contents/metal-materials-and-examples/metal-material-datasheet/werkzeugstahl\\_ms1\\_cx/ms1/ms-ms1-m280\\_m290\\_400w\\_material\\_data\\_sheet\\_05-14\\_en.pdf](http://www.eos.info/03_system-related-assets/material-related-contents/metal-materials-and-examples/metal-material-datasheet/werkzeugstahl_ms1_cx/ms1/ms-ms1-m280_m290_400w_material_data_sheet_05-14_en.pdf)
- [20] Waszkiewicz, S., Fic, M., Perzyk, M. & Szczepanik, J. (1986). *Die and pressure molds*. Warszawa: WNT. (in Polish).
- [21] Piekło, J. (2019). *Application of SLM additive manufacturing method in production of selected cooling system elements in die casting molds*. Kraków: Wydawnictwo Naukowe Akapit. (in Polish).
- [22] Piekło, J. & Maj, M. (2014). Methods of additive manufacturing used in the technology of skeleton castings. *Archives of Metallurgy and Materials*, 2014 ,59, 699-702. DOI: 10.2478/amm-2014-0114.
- [23] Bonderek, Z. & Chromik, S. (2006). *Metal pressure die-casting and plastic injection molding*. Kraków: Wydawnictwo Naukowe Akapit. (in Polish).